

infection. Epidemiological studies of individuals with gastric ulcers demonstrate a higher prevalence of *H. pylori* infections in Le^b-positive individuals (28). In our assay, bacteria only bound to gastric epithelium if Le^b was expressed (Fig. 4).

The Le^b carbohydrates may serve as a therapy for *H. pylori* infections and gastric ulcer disease. Soluble receptor analogs (29) could competitively inhibit pathogenic bacterial attachment without interfering with the indigenous flora, circumventing the negative effects of broad-spectrum antibiotics (30).

The Le^b antigen substituted with a terminal GalNAc α 1-3 residue, A-Le^b [blood group A determinant (Table 1)] (16), did not bind to bacteria in solution (24) nor did it inhibit bacterial adherence in situ. The terminal sugar residues GalNAc α 1-3 (blood group A) or Gal α 1-3 (blood group B) will, in addition to the H antigen, also substitute the Le^b antigen (A-Le^b and B-Le^b, respectively) (16). Thus, there might be fewer available *H. pylori* receptors in individuals of blood group A and B phenotypes, as compared with blood group O individuals. This may explain epidemiological observations (31) that individuals of blood group O phenotype run a greater risk for developing gastric ulcers. Distinctive differences in carbohydrate compositions of natural glycoconjugates are genetically regulated in individuals and populations (18). It is an interesting notion that the glycosylation patterns of soluble glycoconjugates, that is, natural receptor analogs in secretions such as breast milk and saliva (32), may act as clearance factors and consequently govern the susceptibility for bacterial adherence and colonization.

REFERENCES AND NOTES

- Wyatt and M. F. Dixon, *J. Pathol.* **154**, 113 (1988).
- D. Y. Graham, *J. Gastroenterol. Hepatol.* **6**, 105 (1991).
- D. Forman *et al.*, *Lancet* **341**, 1359 (1993).
- N. Akopyanz *et al.*, *Nucleic Acids Res.* **20**, 5137 (1992).
- D. Y. Graham, P. D. Klein, A. R. Opekun, T. W. Boutton, *J. Infect. Dis.* **157**, 777 (1988).
- G. I. Perez-Perez *et al.*, *ibid.* **161**, 1237 (1990).
- N. Sharon, in *The Lectins: Properties, Functions and Applications in Biology and Medicine*, I. E. Liener, N. Sharon, I. J. Goldstein, Eds. (Academic Press, New York, 1986), pp. 494–525.
- K.-A. Karlsson, *Annu. Rev. Biochem.* **58**, 309 (1989).
- D. G. Evans *et al.*, *J. Bacteriol.* **175**, 674 (1993).
- T. Saitoh *et al.*, *FEBS Lett.* **282**, 385 (1991).
- J.-L. Fauchère and M. J. Blaser, *Microb. Pathog.* **9**, 427 (1990).
- P. Falk *et al.*, *Proc. Natl. Acad. Sci. U.S.A.* **90**, 2035 (1993).
- Bacterial in situ adherence assay was as described (12). Human stomach samples were obtained from the Department of Pathology at Washington University. Bacteria were labeled as described (12) or with digoxigenin-3-*O*-succinyl- ϵ -aminocaproic acid *N*-hydroxysuccinimide ester (DIG-NHS; Boehringer Mannheim). Protease inhibitors were included in the labeling reaction; 1 mM phenylmethylsulfonyl fluoride (PMSF), 5 mM EDTA-Na₂, and 10 mM benzamidinium-HCl. Bacterial suspensions were diluted to 0.05 OD₆₀₀ (optical density at 600 nm) in blocking buffer (12), and 200 μ l was applied to the sections, incubated for 1 hour at room temperature, and washed six times for 5 min each in phosphate-buffered saline (PBS) (pH 7.6). DIG-labeled bacteria were then incubated for 1 hour with fluorescein isothiocyanate (FITC)-conjugated sheep antibody to DIG (Boehringer Mannheim) and washed three times for 5 min each in PBS.
- J. Baenziger and S. Kornfeld, *J. Biol. Chem.* **249**, 7260 (1974).
- J. Descamps, M. Monsigny, J. Montreuil, *C. R. Acad. Sci.* **266D**, 1775 (1968).
- H. Clausen and S.-I. Hakomori, *Vox Sang.* **56**, 1 (1989).
- J. Finne *et al.*, *J. Biol. Chem.* **264**, 6720 (1989).
- D. M. Marcus, in *Human Immunogenetics, Basic Principles and Clinical Relevance*, S. D. Litwin, Ed. (Dekker, New York, 1989), pp. 685–699.
- J. C. Paulson and K. J. Colley, *J. Biol. Chem.* **264**, 17615 (1989).
- Human colostrum samples were obtained from Children's Hospital, St. Louis, MO. Colostrum samples were delipidated, and cellular debris was removed by centrifugation two times for 30 min each at 20,000 rpm in a Sorvall SS-34 rotor. SDS-polyacrylamide gel electrophoresis (SDS-PAGE) of human colostrum samples was done with 4 to 20% gels (Bio-Rad), and immunoblots were probed with mAbs to Le^b and Le^a antigens as in Fig. 1.
- The *H. pylori* P466 and WV229 are clinical isolates from patients with acute gastritis and gastric ulcer, respectively.
- We estimated reduction in bacterial binding by counting the number of adherent bacteria in two different fields under magnification $\times 20$ in two independent inhibition experiments. The controls where bacteria were not preincubated with glycoconjugates were defined as 100% binding.
- Binding of *H. pylori* P466 to glycosphingolipids was analyzed on HPTLC plates (Merck Kiesegel 60, EM Separations, Gibbstown, NJ) (33). Isolation, identification, and structural characterization of glycolipids (Table 1) was as described (34).
- Bacterial suspensions (13) were incubated with biotin-labeled (Biotin-X-NHS, Calbiochem, San Diego, CA) Le^b, H-1, H-2, and A-Le^b neoglycoconjugates for 1 hour at room temperature, washed three times in TBS (pH 7.5), and applied in twofold serial dilutions to nitrocellulose with a slot-blotter. Neoglycoconjugates bound to bacteria were detected with peroxidase-labeled Fab's to biotin with ECL detection (Amersham, Arlington Heights, IL).
- The ability of free oligosaccharides to inhibit bacterial adherence in situ was analyzed by preincubation of DIG-labeled *H. pylori* P466 for 3.5 hours at room temperature with oligosaccharides (Table 1). Bacterial suspensions (13) containing the H-1, Le^a, Le^b, Le^x, and Le^y oligosaccharides were added to tissue sections, excluding the prewashing step.
- H. Debray, D. Decout, G. Strecker, G. Spik, J. Montreuil, *Eur. J. Biochem.* **117**, 41 (1981).
- J. Sakamoto *et al.*, *Cancer Res.* **49**, 745 (1989).
- A. Mentis *et al.*, *Epidemiol. Infect.* **106**, 221 (1991).
- W. Weis *et al.*, *Nature* **333**, 426 (1988).
- S. P. Boriello and H. E. Larson, *J. Antimicrob. Chemother.* **7** (suppl. A), 53 (1981).
- C. A. Clarke *et al.*, *Br. Med. J.* **2**, 643 (1955).
- P. Falk, T. Borén, S. Normark, *Methods Enzymol.*, in press.
- G. C. Hansson *et al.*, *Anal. Biochem.* **146**, 158 (1985).
- G. Larson, P. Falk, L. C. Hoskins, *J. Biol. Chem.* **263**, 10790 (1988).
- Blood group antigens were detected in situ with mAbs to the Lewis antigens (Table 1) (ImmuCor) and FITC-conjugated rabbit antibody to mouse immunoglobulins (Dakopatts).
- We thank R. Gilman of Johns Hopkins University for the *H. pylori* strain P466 and T. U. Westblom of St. Louis University Medical Center for the *H. pylori* strain WV229. Supported by grants from Symbicor (Umeå, Sweden) (S.N.), Public Health Service Fogarty International Research Fellowship (Nr. TW04669-02, number 1430653611A1), the Swedish Society of Medicine (T.B.), the Swedish Institute, the Swedish Medical Research Council (T.B. and P.F.), and the William F. Keck Foundation (P.F.).

23 July 1993; accepted 5 November 1993

Separate GTP Binding and GTPase Activating Domains of a G α Subunit

David W. Markby, René Onrust, Henry R. Bourne*

Most members of the guanosine triphosphatase (GTPase) superfamily hydrolyze guanosine triphosphate (GTP) quite slowly unless stimulated by a GTPase activating protein or GAP. The α subunits (G α) of the heterotrimeric G proteins hydrolyze GTP much more rapidly and contain an ~ 120 -residue insert not found in other GTPases. Interactions between a G α insert domain and a G α GTP-binding core domain, both expressed as recombinant proteins, show that the insert acts biochemically as a GAP. The results suggest a general mechanism for GAP-dependent hydrolysis of GTP by other GTPases.

Heterotrimeric G proteins couple cell surface receptors to intracellular signaling pathways through a GTP-dependent cycle in which α and $\beta\gamma$ subunits regulate effectors (1–3). G α subunits belong to a large, diverse family of GTPases whose members include Ras, the product of the *ras* proto-

oncogenes, and bacterial elongation factor Tu (EF-Tu). GTPase family members share conserved structures and mechanisms: a core GTP-binding domain probably similar in topology to the α - β folds of Ras and EF-Tu and a GTPase cycle that controls protein-protein interactions (3, 4). In the GTPase cycles of all these proteins, exchange of GTP for bound guanosine diphosphate (GDP) initiates activation and GTP hydrolysis terminates activation. For individual GTPases, either of these two

Departments of Pharmacology and Medicine, Cell Biology Program, and Cardiovascular Research Institute, University of California, San Francisco, CA 94143.

*To whom correspondence should be addressed.

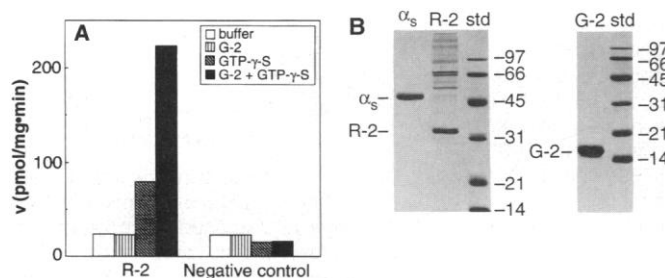
R201 mutations, the Q227L mutation inhibits GTP hydrolysis and constitutively activates α_s (17, 18). Although expression of neither R-1-Q227L nor G-2 alone affected cAMP production, co-expression of both proteins increased the amount of cAMP produced ~ 4.5 -fold (18A); the increase in the amount of cAMP was 25 to 50% of that observed after transfecting equal amounts of DNA encoding wild type α_s . The shortest Gail construct that retained high activity, G-2, encodes 23 COOH-terminal residues that are also encoded in R-1 (Fig. 1B); many of the overlapping residues in G-2 also form part of the proposed Ras-like domain (see Fig. 1).

Prompted by the results in COS-7 cells, we assessed the abilities of Ralph and Gail derivatives, alone or in combination, to stimulate cAMP synthesis in vitro. We used the standard assay for α_s (19)—GTP- γ -S-dependent stimulation of adenylyl cyclase in membranes prepared from S49 *cyc*⁻ cells, which lack endogenous α_s (20). Active R-1

was poorly expressed in *Escherichia coli* without G-2. A second Ralph construct, R-2 (Fig. 1, B and C), retained the ability to stimulate cAMP synthesis in *cyc*⁻ membranes when independently expressed in *E. coli* and mixed with GTP- γ -S and purified G-2. R-2 differs from R-1 both by containing a larger deletion ($\Delta 69$ –203 for R-2, $\Delta 73$ –194 for R-1) and by insertion of a short linker sequence (SGQQG) that is not present in R-1 (Fig. 1, B and C). These changes delete R201 and a stretch of surrounding hydrophobic residues, substituting a shorter hydrophilic sequence that may be more compatible with an exposed loop.

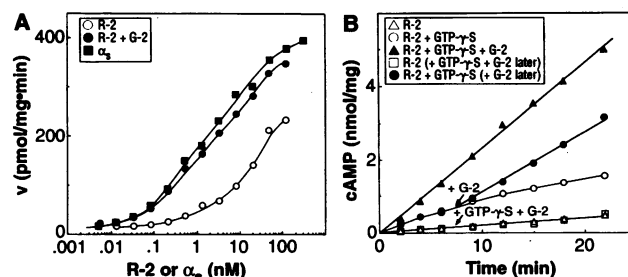
To obtain larger amounts of protein, we partially purified R-2 tagged at the NH₂-terminus with hexahistidine (H₆-R-2) from Sf9 cells after co-expression with G-2 (Fig. 2) (21). For the sake of brevity, we refer hereafter to R-2 and α_s without the H₆ prefix, although all in vitro characterizations of both proteins were done with hexahistidine-tagged proteins.

Fig. 2. Preparation of R-2 and G-2. (A) Stimulation of adenylyl cyclase in vitro. R-2 was partially purified from Sf9 cells co-expressing H₆-R-2 and G-2 (44); the concentration of R-2 in the assay was 5 nM, as assessed by GTP- γ -S binding (44). The negative control sample was obtained from identically processed Sf9 cells expressing G-2. Samples were assayed for stimulation of adenylyl cyclase activity in S49 *cyc*⁻ membranes as described (18) with some modifications: The reaction buffer was 50 mM Na-Hepes (pH 8.0) and MgCl₂ was at 5 mM. Forskolin (10 μ M) was included in all assays, and 100 μ M GTP- γ -S and 2.5 μ M G-2 were added as indicated. Membranes (30 μ g per tube) were incubated for 2 min at 30°C with activators and soluble protein samples. Reactions, in a total volume of 0.1 ml, were initiated by the addition of ATP and cAMP and terminated after 10 min with 0.5% SDS. Each point is the mean of duplicate determinations. (B) SDS-polyacrylamide gels of R-2, α_s , and G-2. Proteins were resolved by SDS-polyacrylamide gel electrophoresis (PAGE) (12.5% gel for R-2 and α_s ; 15% gel for G-2), then gels were stained with Coomassie Blue. The positions of R-2, α_s , G-2, and the molecular size standards (std) are noted. The identity of the purified proteins was confirmed by protein immunoblotting with monoclonal antibody 12CA5 (for G-2) or affinity-purified rabbit polyclonal antisera to residues 27 to 41 of α_s (for R-2 and α_s) (45).



Each point is the mean of duplicate determinations. (B) SDS-polyacrylamide gels of R-2, α_s , and G-2. Proteins were resolved by SDS-polyacrylamide gel electrophoresis (PAGE) (12.5% gel for R-2 and α_s ; 15% gel for G-2), then gels were stained with Coomassie Blue. The positions of R-2, α_s , G-2, and the molecular size standards (std) are noted. The identity of the purified proteins was confirmed by protein immunoblotting with monoclonal antibody 12CA5 (for G-2) or affinity-purified rabbit polyclonal antisera to residues 27 to 41 of α_s (for R-2 and α_s) (45).

Fig. 3. Adenylyl cyclase stimulation by R-2, the complex of R-2 and G-2, and α_s . (A) Dependence of effect on concentration. Assays were done as described (Fig. 2A). Forskolin (10 μ M) was included in all samples, and 100 μ M GTP- γ -S and 2.5 μ M G-2 were added as indicated. Before the assay, α_s and R-2 were incubated with 100 μ M GTP- γ -S and 5 mM MgCl₂ in HEB with bovine serum albumin (100 μ g/ml), then serially diluted in the same buffer and held on ice. Incubation was for 60 min at 20°C for α_s and for 30 min on ice for R-2. (B) Time courses of cAMP production. Assays were done as in Fig. 3A, except that R-2 was not preactivated with GTP- γ -S, and portions (50 μ l) were withdrawn from a large-scale reaction for each time point. Forskolin (10 μ M) was included in all samples, and 100 μ M GTP- γ -S and 2.5 μ M G-2 were added as indicated.



Before the assay, α_s and R-2 were incubated with 100 μ M GTP- γ -S and 5 mM MgCl₂ in HEB with bovine serum albumin (100 μ g/ml), then serially diluted in the same buffer and held on ice. Incubation was for 60 min at 20°C for α_s and for 30 min on ice for R-2. (B) Time courses of cAMP production. Assays were done as in Fig. 3A, except that R-2 was not preactivated with GTP- γ -S, and portions (50 μ l) were withdrawn from a large-scale reaction for each time point. Forskolin (10 μ M) was included in all samples, and 100 μ M GTP- γ -S and 2.5 μ M G-2 were added as indicated.

Partially purified R-2 with GTP- γ -S stimulated cAMP production in *cyc*⁻ membranes, even in the absence of G-2; stimulation was increased by addition of purified G-2, however (Fig. 2A). Neither G-2 alone nor a control preparation from Sf9 cells showed stimulatory activity (Fig. 2A). Because attempts to purify R-2 further were frustrated by low amounts of expression and instability of the protein, we characterized the partially purified preparation (Fig. 2B) (21). G-2 was abundantly expressed in *E. coli* and was stable during purification (Fig. 2) and assay.

The concentration effect curves for activation of adenylyl cyclase in the presence of GTP- γ -S and forskolin were remarkably similar for the complex of R-2 and G-2 and for intact α_s (Fig. 3A): concentrations of R-2 and α_s required for half-maximal activation were ~ 3 nM and ~ 2 nM, respectively; both proteins stimulated adenylyl cyclase to similar maximal extents (350 to 400 pmol/min per milligram of *cyc*⁻ membrane). The concentration effect curve for R-2 and G-2 was obtained in the presence of a saturating concentration of G-2 (2.5 μ M). The concentration of G-2 that gave half-maximal activation of adenylyl cyclase ($K_{0.5}$) was ~ 25 nM in the presence of 2 nM R-2.

In the presence of G-2 and GTP- γ -S the concentration of R-2 required to stimulate adenylyl cyclase was 1/20 of that required to stimulate adenylyl cyclase in the presence of GTP- γ -S alone (Fig. 3A). The apparent cooperation between R-2 and G-2 in stimulating adenylyl cyclase in vitro is reminiscent of the results in COS-7 cells, where the effect of R-1-Q227L on cAMP synthesis required co-expression with G-2. GTP- γ -S-dependent cAMP synthesis for R-2 plus G-2 was linear with time, but nonlinear without G-2; if G-2 was added during the reaction, cAMP synthesis increased, but not to the rate observed when G-2 was present from the start of the reaction (Fig. 3B). Thus, in the presence of GTP- γ -S, G-2 apparently protects R-2 from inactivation and also stabilizes a conformation that efficiently stimulates adenylyl cyclase. If R-2 was incubated in the absence of GTP- γ -S, very little activity was detected upon later addition of GTP- γ -S and G-2 (Fig. 3B). Thus, GTP- γ -S alone also partially stabilizes R-2 against denaturation.

An alternative explanation for Ralph-Gail cooperation—that the Gail domain contains a contact site for adenylyl cyclase—seems unlikely. R-2 activates adenylyl cyclase in the absence of G-2, and G-2 is an inactive (or very weak) competitive inhibitor (inhibition constant, $K_i > 500$ μ M) of α_s -dependent stimulation (22). Furthermore, all the known regions of α_s in which amino acid replacements impair stimulation of adenylyl cyclase map to a face of the Ras-like domain directly oppo-

site to the location of Gail in our G_α model (10, 12, 23).

Measurements of adenylyl cyclase activity showed that R-2 bound GTP- γ -S in the absence of G-2. The postulated position of the insert domain (Fig. 1) suggests, however, that it may contribute both to GTP binding and to GTP hydrolysis.

In filtration binding assays (Fig. 4) G-2 promoted tight binding of GTP- γ -S to R-2, whereas R-2 alone bound GTP- γ -S relatively weakly. Saturating concentrations of G-2 increased the amount of GTP- γ -S bound by R-2 preparations by ~12-fold at 400 nM GTP- γ -S (Fig. 4A) (24). G-2 alone showed no detectable binding of GTP- γ -S. For G-2, the $K_{0.5}$ for promoting high-affinity binding was 50 nM (Fig. 4A), and the concentration of GTP- γ -S required for half-maximal binding to the complex of R-2 and G-2 was 15 nM (Fig. 4B). These apparent affinities presumably reflect formation of a stable R-2 · G-2 · GTP- γ -S · Mg²⁺ complex. Consistent with this interpretation, GTP- γ -S dissociated from R-2 and G-2 slowly but measurably under these conditions (half-time, $t_{1/2} \cong 170$ min); without glycerol, dissociation was more rapid [$t_{1/2} \cong 10$ min (18a)]. By contrast, dissociation of Mg²⁺ · GTP- γ -S from α_s was undetectable under both conditions [(Fig. 4C) (18a)]. GTP- γ -S bound much more rapidly to the complex of R-2 and G-2 ($t_{1/2} \cong 0.4$ min) than to intact α_s ($t_{1/2} \cong 45$ min) (Fig. 4D) (25). Because isolated G_α subunits contain bound GDP, and the rate of GDP dissociation determines the rate of GTP- γ -S binding (26), we infer that the complex of R-2 and G-2 binds GDP much less tightly than does α_s (27).

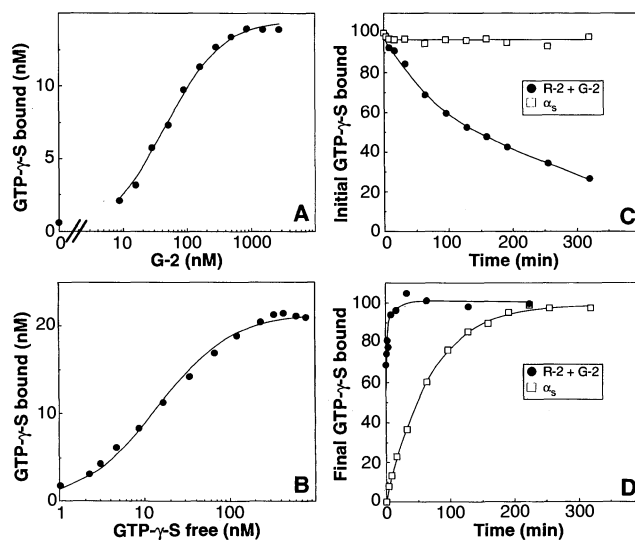
To test the proposal that G-2 accelerates GTP hydrolysis by R-2, we measured steady-state GTPase rates: G-2 stimulated the GTPase activity of R-2 preparations under conditions where neither R-2 nor G-2 alone hydrolyzed GTP (Fig. 5A). If G-2 was added during the R-2 time course, the rate of phosphate release equaled the initial rate measured for in the presence of R-2 and G-2 (Fig. 5A). Thus, R-2 was stable under GTPase assay conditions, and G-2 did not stimulate activity simply by preventing denaturation of R-2. Under these conditions, the initial velocity divided by the concentration of R-2 ($v_i/[R-2]$) was approximately 2 min⁻¹ and was constant over the range 8 to 30 nM R-2. The rate of GTP hydrolysis by R-2 alone was very low, and difficult to measure accurately; from assays at 100 nM of R-2, we estimate that G-2 stimulates R-2 activity at least 100-fold at 1 μ M GTP (24). GTP hydrolysis by G-2 alone was undetectable even at a saturating concentration of G-2 (10 μ M). The concentration of G-2 required for half-maximal stimulation of GTP

hydrolysis was ~1 μ M; this is severalfold higher than the concentrations required for GTP- γ -S binding or stimulation of adenylyl cyclase ($K_{0.5} \cong 25$ to 50 nM).

GTP hydrolysis by the complex of R-2 and G-2 followed Michaelis-Menten kinetics with a Michaelis constant, K_m , of 150 nM and $V_{max}/[R-2]$ of 2.3 min⁻¹ (Fig. 5B). The steady-state GTPase activity of the R-2 and G-2 complex was much greater than

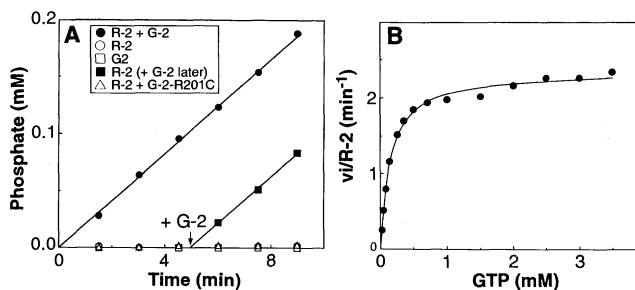
that of α_s ($v_i/[\alpha_s] \cong 0.015$ min⁻¹ and 0.05 min⁻¹, with and without glycerol, respectively). This disparity reflects the relatively slow dissociation of GDP from α subunits, which is largely rate limiting for both steady-state GTP hydrolysis (28) and GTP- γ -S binding (26). By contrast, the rate of hydrolysis of GTP bound to α_s ($k_{cat,GTP}$) is much faster, at 4 min⁻¹ (29). The maximal steady-state GTPase rate of the complex of

Fig. 4. Binding of GTP- γ -S to the complex of R-2 and G-2. (A) Dependence of GTP- γ -S binding on G-2. GTP- γ -S binding was quantitated by nitrocellulose filter binding assays (48). Reactions included 14 nM R-2, 400 nM GTP- γ -S, and various concentrations of G-2. R-2 and G-2 were preincubated at 20°C in buffer G [50 mM Na-Hepes (pH 8.0), 1 mM EDTA, 2 mM 2-mercaptoethanol, 10 mM MgSO₄, 2 mM adenosine triphosphate (ATP), 30% glycerol, and bovine serum albumin (1 mg/ml)] for 2 min. Reactions were initiated by addition of [³⁵S]GTP- γ -S (~500,000 cpm per 50 μ l). The incubation was continued for 30 min and terminated by addition of 1 ml of ice-cold stop buffer [20 mM tris-Cl (pH 8.0), 25 mM MgCl₂, 100 mM NaCl]. Samples were immediately filtered thru BA85 filters and washed twice with ~6 ml of stop buffer. Filters were removed from aspiration within a few minutes, and bound GTP- γ -S was quantitated by liquid scintillation counting. G-2 alone showed no detectable GTP- γ -S-binding activity. Buffer G includes glycerol and bovine serum albumin to stabilize R-2 (Fig. 5A), ATP to inhibit non-specific GTPase activity present in some samples, and 10 mM MgSO₄ to promote high-affinity GTP- γ -S binding and GTPase activity. (B) GTP- γ -S concentration curve. Reactions were performed as in (A) except that R-2 and G-2 were fixed at 22 nM and 2.5 μ M, respectively, and the total concentration of GTP- γ -S was varied. The concentration of free GTP- γ -S was determined by subtraction of bound from total ligand. (C) Time courses of GTP- γ -S dissociation. [³⁵S]GTP- γ -S (400 nM) was incubated at 20°C in buffer G with 10 nM R-2 and 5 μ M G-2 for 5 min or with 10 nM α_s for 200 min. Dissociation measurements of bound [³⁵S]GTP- γ -S were initiated by adding 200 μ M unlabeled GTP- γ -S and portions (50 μ l) were withdrawn from a larger reaction to follow the time course. (D) Time courses of GTP- γ -S association. Experiments were done as in (A) except that a time course was followed by withdrawing portions (50 μ l) from a large-scale reaction. Assays included 10 nM R-2 and 5 μ M G-2 or 10 nM α_s , as appropriate.



of ice-cold stop buffer [20 mM tris-Cl (pH 8.0), 25 mM MgCl₂, 100 mM NaCl]. Samples were immediately filtered thru BA85 filters and washed twice with ~6 ml of stop buffer. Filters were removed from aspiration within a few minutes, and bound GTP- γ -S was quantitated by liquid scintillation counting. G-2 alone showed no detectable GTP- γ -S-binding activity. Buffer G includes glycerol and bovine serum albumin to stabilize R-2 (Fig. 5A), ATP to inhibit non-specific GTPase activity present in some samples, and 10 mM MgSO₄ to promote high-affinity GTP- γ -S binding and GTPase activity. (B) GTP- γ -S concentration curve. Reactions were performed as in (A) except that R-2 and G-2 were fixed at 22 nM and 2.5 μ M, respectively, and the total concentration of GTP- γ -S was varied. The concentration of free GTP- γ -S was determined by subtraction of bound from total ligand. (C) Time courses of GTP- γ -S dissociation. [³⁵S]GTP- γ -S (400 nM) was incubated at 20°C in buffer G with 10 nM R-2 and 5 μ M G-2 for 5 min or with 10 nM α_s for 200 min. Dissociation measurements of bound [³⁵S]GTP- γ -S were initiated by adding 200 μ M unlabeled GTP- γ -S and portions (50 μ l) were withdrawn from a larger reaction to follow the time course. (D) Time courses of GTP- γ -S association. Experiments were done as in (A) except that a time course was followed by withdrawing portions (50 μ l) from a large-scale reaction. Assays included 10 nM R-2 and 5 μ M G-2 or 10 nM α_s , as appropriate.

Fig. 5. GTPase activity of the complex of R-2 and G-2. (A) Time courses of GTP hydrolysis. GTPase activity was measured as the production of free [³²P]phosphate from [³²P]GTP, as described (28) with some modifications. Reactions contained 1 μ M GTP and 10 nM R-2, 10 μ M G-2, or 10 μ M G-2-R201C, as indicated. Proteins were incubated for 2 min at 20°C in G buffer, and reactions were initiated by the addition of [³²P]GTP (~500,000 cpm per 50- μ l reaction). Reactions were terminated and protein-dependent phosphate release was quantitated as described (28). (B) GTP saturation curve. Reaction conditions were as in (A) except that the GTP concentration was varied, and the ATP concentration in buffer G was reduced to 200 μ M. Reactions included 10 nM R-2 and 10 μ M G-2. Each data point represents the mean of triplicate determinations at a fixed time point where product formation was linear with time (1 to 10 min, depending on the substrate concentration).



R-2 and G-2 (2.3 min^{-1}) places a lower limit on both $k_{\text{cat,GTP}}$ and the rate of GDP dissociation. Thus, $k_{\text{cat,GTP}}$ for the complex of R-2 and G-2 is comparable to reported values for α_s , and may even be greater. In addition, GDP dissociation from the complex of R-2 and G-2 must be manyfold faster than that from α_s , a difference also reflected in the relative rates of GTP- γ -S binding (Fig. 4D), which we also attribute to different rates of GDP release.

We constructed a mutant G-2 in which the arginine was replaced by cysteine; this R201C mutation was the most frequent mutation found in the *gsp* oncogenes of pituitary tumors (8). We predicted that R-2 complexed with the mutant G-2 would behave like the corresponding mutant α_s : it would hydrolyze GTP slowly, bind GTP in a stable fashion, and consequently respond to activation by GTP as it responds to activation by the hydrolysis-resistant GTP analog, GTP- γ -S. Indeed, G-2-R201C stimulated GTP hydrolysis by R-2 very weakly (Fig. 5A); in assays performed at a 10-fold higher R-2 concentration and 1 μM GTP, the mutant G-2 increased GTPase activity of the R-2 preparation only two-fold, in contrast to the 100-fold stimulation seen with unmodified G-2.

Steady-state binding measurements confirmed the GTPase measurements, by showing that R-2 complexed with G-2-R201C stably binds GTP but hydrolyzes it inefficiently (Fig. 6A). Under the conditions of the GTPase assay, R-2 complexed to G-2-R201C bound both [^{35}S]GTP- γ -S and [γ - ^{32}P]GTP ($\sim 85\%$ and $\sim 70\%$, respectively, of the amount of [^{35}S]GTP- γ -S bound by R-2 complexed with G-2). In contrast, R-2 with G-2 retained a relatively small amount of [γ - ^{32}P]GTP ($\sim 15\%$ of the amount of bound [^{35}S]GTP- γ -S). The differences in [γ - ^{32}P]GTP binding presumably reflect differences in the rates of GTP hydrolysis and release of [^{32}P]phosphate in the presence of normal and modified G-2.

Both GTP- γ -S and GTP supported stimulation of adenylyl cyclase by R-2 complexed to G-2-R201C under conditions where activation by R-2 complexed to G-2 was much

greater with GTP- γ -S than with GTP (Fig. 6B). R-2 was only slightly active in the absence of G-2 because its concentration was relatively low in these experiments.

Thus, for both the complex of R-2 and G-2 and intact α_s , the R201C mutation inhibits GTP hydrolysis and promotes GTP-dependent stimulation of the effector. Although G-2 clearly increases the affinity of R-2 for GTP- γ -S and presumably for GTP, the biochemical behavior of G-2-R201C indicates that G-2 normally accelerates hydrolysis of bound GTP apart from increasing affinity for substrate (25).

Separate expression of R-2 and G-2 and the biochemical properties of the resulting fragments strongly support a key tenet of our $G\alpha$ model—that Ralph and Gail are separate domains, structurally and functionally. The ability of R-2 alone to stimulate adenylyl cyclase in the presence of GTP- γ -S (Fig. 3A) indicates that the Ralph domain is the GTP-binding core of $G\alpha$, although G-2 does increase the affinity of R-2 for binding GTP- γ -S. The Gail domain is a stably folded protein with appreciable secondary and tertiary structure, as judged by circular dichroism (18A) and heteronuclear nuclear magnetic resonance spectroscopy of G-2 (30). Biochemical interactions of Ralph and Gail as separate fragments probably represent interactions of these domains in the intact $G\alpha$ protein: G-2 stabilized R-2 from thermal inactivation (Fig. 3B), increased its affinity for binding GTP- γ -S (Fig. 4) and its apparent affinity for stimulating adenylyl cyclase (Fig. 3), and also stimulated GTP hydrolysis (Fig. 5A).

Functional and structural similarities between $G\alpha$ chains and small GTPases (3) suggest that these protein families evolved from a common ancestor. The covalent attachment of a GAP-like domain to the GTPase core of $G\alpha$ may represent an example of exon shuffling in evolution (31). The human genes for α_s and three α_i species (32) contain a splice site at codon 220 (α_s numbering), very near the COOH-terminus of Gail, as defined functionally, but within the proposed α/β fold of Ralph. In α_s , splice junctions also flank the predicted Gail structural domain.

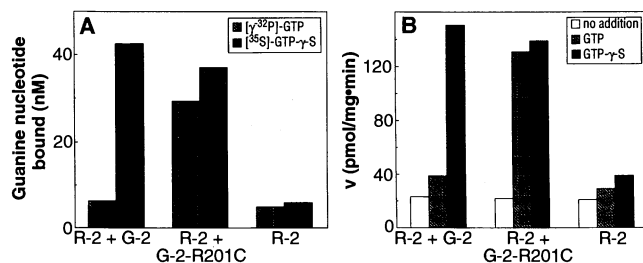
The biochemical interactions of R-2 and G-2 suggest that their interactions involve both interdomain contacts and also direct interactions of residues from the two fragments with bound nucleotide. Clearly, GTP- γ -S binding and association of R-2 and G-2 are functionally linked: G-2 promoted tight binding of GTP- γ -S in the presence of Mg^{2+} (Fig. 4A), whereas GDP dissociated relatively rapidly; similarly, during purification in the presence of GDP, excess G-2 was readily separated from R-2 bound to a Ni^{2+} column (Fig. 2B), but in the presence of GTP- γ -S, the column partially retained G-2 along with R-2 (18A). We suspect that G-2 interacts with bound Mg^{2+} and the phosphates of GTP- γ -S (and GTP) through T204 and R201. However, R201 is not necessary for GTP- γ -S-dependent interaction between R-2 and G-2 (Fig. 6).

R-2 and G-2 represent an unusual example of complementation between protein fragments, in that Gail is an insert within Ralph that can be supplied exogenously. The finding that deletion of residues 211 to 217 from G-2 prevented it from cooperating effectively with Ralph was unexpected because these residues form the external $\beta 2$ strand of the Ras-like domain in our model and are also present in both R-1 and R-2 (see Fig. 1). In other systems, complementing protein fragments frequently contain overlapping sequences whose role is similarly obscure (33). The redundant residues of G-2 could interact with R-2 in several ways—by replacing the corresponding amino acids of R-2 in the α/β fold, by forming an additional β strand that extends the β sheet, or by stabilizing the conformation of the COOH-terminus of G-2 itself.

Despite the absence of covalent links between R-2 and G-2, the two polypeptides together hydrolyze GTP quite rapidly. Under steady-state conditions, the complex of R-2 and G-2 hydrolyzes GTP much more rapidly than does α_s , owing to faster dissociation of GDP from the complex of R-2 and G-2 than from α_s . In this respect, the GAP activity of G-2 differs from that of other GAPs: GTPase stimulation by G-2 can be observed at steady-state in the absence of the guanine nucleotide exchange proteins that catalyze GDP dissociation from other GTPases.

Structural and functional similarities support the analogy between the $G\alpha$ insert and Ras-GAP: G-2 is a GAP for R-2; GTP- γ -S promotes interaction between R-2 and G-2, just as GTP binding promotes tight binding of GAP to Ras (13); the GTP-binding domains of $G\alpha$ and Ras probably share a similar fold, and the topological location of Gail in the $G\alpha$ model is identical to the GAP-binding region of Ras. $G\alpha$ insert domains and Ras-GAPs also both contain conserved arginine residues

Fig. 6. Characterization of G-2-R201C. (A) Fractional saturation with GTP- γ -S and GTP. Steady-state binding of [^{35}S]GTP- γ -S and [γ - ^{32}P]GTP was measured as described in Fig. 4A, except that the reaction time was 5 min and filters were washed only once. Nucleotides, 1 μM ; R-2, 40 nM; G-2 or G-2-R201C, 10 μM . Data are means of duplicate determinations. (B) GTP-dependent stimulation of adenylyl cyclase. Adenylyl cyclase activity was measured as in Fig. 3A, without preactivation by nucleotides. Conditions were 10 μM forskolin, 1 nM R-2, 10 μM G-2 or G-2-R201C, and 100 μM GTP or GTP- γ -S. Bars show the mean of duplicate determinations.



that may participate directly in catalysis.

Although high-resolution structures have been determined for both Ras (34, 35) and EF-Tu (36), the mechanism of GTP hydrolysis by these proteins remains obscure (37). Neither Ras nor EF-Tu hydrolyzes GTP very efficiently in the absence of its respective GAP. By contrast, $G\alpha$ subunits and the complex of R-2 and G-2 hydrolyze GTP more rapidly and may offer a clue to the catalytic mechanism of other GAP-GTPase complexes. In general, GAPs could stimulate GTP hydrolysis by promoting a conformational change in the GTPase core, by providing active site residues, or by a combination of these effects.

Arginine 201 of α_s , a residue conserved in the Gail region of all known $G\alpha$ subunits, may participate directly in GTP hydrolysis. Replacements of R201 in α_s by Ala, Lys, Glu, His, or Cys all greatly reduce $k_{cat,GTP}$ (8, 9); similarly, an R201C mutation in G-2 inhibited hydrolysis of GTP bound to the complex of R-2 and G-2 (Fig. 6A). Of several possible mechanisms for catalysis by GAPs (37), one plausible role for an active site arginine is to stabilize the negative charge developed in a pentavalent transition state after nucleophilic attack of water at the γ -phosphate.

By analogy with $G\alpha$ subunits, members of the Ras-GAP family may stimulate GTPase activity through a catalytic arginine residue corresponding to R903 of Ras-GAP (38). The possibility that amino acids from Ras-GAP participate directly in catalysis is structurally feasible because the γ -phosphate of GTP bound to Ras is accessible to side chains of residues of another protein (35). Mutational data are consistent with a catalytic role for R903 of Ras-GAP: two substitutions, R903K and L902I, reduce GTPase stimulation to less than 1/30 and 1/200 that of the wild-type protein, respectively, without large effects on affinity for GTP-bound Ras, whereas the R903E mutation reduces GAP activity to less than 1/5000 that of the wild-type protein, with an affinity for activated Ras 1/15 that of wild-type GAP (38). Potential structural similarities between the Gail domain of $G\alpha$ and GAPs for other GTPases are difficult to identify, in view of the low sequence similarity between $G\alpha$ chains and Ras-GAPs and the diversity in primary structure of GAPs for different GTPases (39).

The Gail domain of $G\alpha$ may interact with other signaling proteins. Such proteins could include certain effectors that are reported to accelerate GTP hydrolysis by $G\alpha$ (6). We prefer instead to imagine that these effectors accelerate GTP hydrolysis via allosteric changes induced in the GTPase core of $G\alpha$, because all the available evidence for $G\alpha$ -effector interaction regions

points to residues on a face of the GTPase core domain directly opposite to the location of Gail in our $G\alpha$ model (10).

REFERENCES AND NOTES

1. A. G. Gilman, *Annu. Rev. Biochem.* **56**, 615 (1987).
2. L. Birnbaumer, *Cell* **71**, 1069 (1992).
3. H. R. Bourne, D. A. Sanders, F. McCormick, *Nature* **348**, 125 (1990); *ibid.* **349**, 117 (1991).
4. Y. Kaziro, H. Itoh, T. Kozasa, M. Nakafuku, T. Satoh, *Annu. Rev. Biochem.* **60**, 349 (1991).
5. We refer to the rate constant for hydrolysis of bound GTP as $k_{cat,GTP}$, to be consistent with terminology in the G protein field. This term should not be confused with k_{cat} , which is V_{max} divided by the concentration of enzyme sites.
6. G. Berstein *et al.*, *Cell* **70**, 411 (1992); V. Y. Arshavsky and M. D. Bownds, *Nature* **357**, 416 (1992).
7. G. A. Martin *et al.*, *Cell* **63**, 843 (1990); P. Gideon *et al.*, *Mol. Cell. Biol.* **12**, 2050 (1992); J. F. Eccleston, D. B. Dix, R. C. Thompson, *J. Biol. Chem.* **260**, 16237 (1985).
8. C. A. Landis *et al.*, *Nature* **340**, 692 (1989).
9. M. Freissmuth and A. G. Gilman, *J. Biol. Chem.* **264**, 21907 (1989).
10. C. H. Berlot and H. R. Bourne, *Cell* **68**, 911 (1992).
11. B. R. Conklin and H. R. Bourne, *ibid.* **73**, 631 (1993).
12. H. Itoh and A. G. Gilman, *J. Biol. Chem.* **266**, 16226 (1991); H. M. Farick, N. O. Artemyev, H. E. Hamm, *Science* **256**, 1031 (1992).
13. G. Bollag and F. McCormick, *Annu. Rev. Cell Biol.* **7**, 601 (1991); P. Polakis and F. McCormick, *J. Biol. Chem.* **268**, 9157 (1993).
14. D. Cassel and Z. Selinger, *Proc. Natl. Acad. Sci. U.S.A.* **74**, 3307 (1977); C. Van Dop, M. Tsubokawa, H. R. Bourne, J. Ramachandran, *J. Biol. Chem.* **259**, 696 (1984).
15. J. Lyons *et al.*, *Science* **249**, 655 (1990).
16. Y. H. Wong *et al.*, *Nature* **351**, 63 (1991); Y. H. Wong, B. R. Conklin, H. R. Bourne, *Science* **255**, 339 (1992); B. R. Conklin *et al.*, *J. Biol. Chem.* **267**, 31 (1992).
17. M. P. Graziano and A. G. Gilman, *J. Biol. Chem.* **264**, 15475 (1989).
18. S. B. Masters *et al.*, *ibid.*, p. 15467.
- 18a. D. W. Markby, R. Onrust, H. R. Bourne, unpublished data.
19. Assays included forskolin, which binds directly to adenylyl cyclase, stimulates cAMP synthesis, and increases the apparent affinity of the enzyme for α_s . At the concentration used (10 μ M), forskolin decreased the $K_{0.5}$ for α_s as a stimulator of cAMP production \sim 100-fold.
20. H. R. Bourne, P. Coffino, G. M. Tomkins, *Science* **187**, 750 (1975); B. A. Harris, J. D. Robishaw, S. M. Mumby, A. G. Gilman, *ibid.* **229**, 1274 (1985).
21. Impurities in the sample are unlikely to have substantially affected the results, because the assays are either specific for α_s activity (GTP-dependent adenylyl cyclase stimulation) or largely dependent on the addition of G-2 (GTP- γ -S binding and GTPase). The R-2 preparation was not contaminated with either G-2 or endogenous α_s from Sf9 cells, as indicated by the following observations: (i) Complementation by G-2 in the *cyc*⁻ assay was similar for R-2, whether it was derived from Sf9 cells expressing R-2 and G-2 or from *E. coli* expressing R-2 alone. (ii) An identically processed control from Sf9 cells expressing G-2 alone gave no stimulation of cAMP production (Fig. 2A). (iii) R-2 was largely inactivated by a 5-min incubation at 30°C in the absence of GTP- γ -S (Fig. 3B), whereas α_s was stable under these conditions. (iv) Neither α_s nor G-2 was detected in the sample by protein immunoblotting.
22. The $K_{0.5}$ for GTP- γ -S-dependent adenylyl cyclase stimulation was about 20-fold greater for R-2 than for the complex of R-2 and G-2 or α_s ; part of this difference was due to the instability of R-2 (Fig. 3, A and B). G-2 (100 μ M) had no effect on the $K_{0.5}$ for stimulation of adenylyl cyclase by α_s . GTP- γ -S in *cyc*⁻ membranes or on stimulation by the β -adrenoceptor agonist isoproterenol in wild-type S49 membranes.
23. S. B. Masters *et al.*, *Science* **241**, 448 (1988).
24. We do not know whether the low GTP- γ -S binding and GTPase activities of the R-2 preparation in the absence of G-2 were due to R-2 itself. About 50 to 80% of the activity was not due to R-2 as judged from assays of a control from Sf9 cells (Fig. 2A) or R-2 incubated at 30°C for 15 min; both samples exhibited low activity that was not further stimulated by added G-2.
25. An alternative explanation for the effect of G-2 on the rate of GTP- γ -S binding and steady-state GTPase is that R-2 binds GDP rather tightly and that G-2 accelerates GDP release. This interpretation is unlikely, because it is hard to imagine how the changes created in the GDP or GTP binding site by converting α_s into R-2 would increase affinity for binding GDP. Also, R-2 binds GTP- γ -S rapidly and stoichiometrically in the absence of G-2: GTP- γ -S (100 μ M) protected R-2 from inactivation during incubation at 30°C for 2 min or at 20°C for 15 min, in HEB buffer with 10 mM MgCl₂, as assessed by subsequent assays of adenylyl cyclase stimulation with added GTP- γ -S and G2. In the presence of GTP- γ -S, greater than 80% of R-2 activity remained after such incubation, whereas in the absence of GTP- γ -S, less than 10% of R-2 activity remained. Furthermore, G-2-R201C promoted GTP binding but not rapid hydrolysis (Fig. 6A), implying that G-2 does not increase steady-state GTPase of R-2 by catalyzing GDP release.
26. K. M. Ferguson, T. Higashijima, M. D. Smigel, A. G. Gilman, *J. Biol. Chem.* **261**, 7393 (1986).
27. In the case of $G\alpha$ subunits, GTP- γ -S binding follows first order kinetics, with an observed rate constant that is equal to the rate constant for GDP dissociation. Although the rapid binding of GTP- γ -S to the complex of R-2 and G-2 indicates that GDP dissociates readily from this complex, this approach cannot measure precisely the rate of GDP release from the complex of R-2 and G-2 because the kinetic pathway for GTP- γ -S binding is unknown and the data (Fig. 4D) are not well described by a single exponential and are imprecise, owing to the rapidity of GTP- γ -S binding. The slow rate of GTP- γ -S binding to α_s under these conditions is partially due to glycerol, which inhibits GDP release from α chains (26); the observed rate constants with and without glycerol are 0.015 min⁻¹ and 0.05 min⁻¹, respectively. The value without glycerol is slower than those for the long and short splice variants of α_s , 0.3 min⁻¹ and 0.1 min⁻¹, respectively [M. P. Graziano, M. Freissmuth, A. G. Gilman, *J. Biol. Chem.* **264**, 409 (1989)]. Several factors may account for this discrepancy including the hexahistidine tag, the source of protein, or solution conditions.
28. T. Higashijima, K. M. Ferguson, M. D. Smigel, A. G. Gilman, *J. Biol. Chem.* **262**, 757 (1987).
29. M. P. Graziano, M. Freissmuth, A. G. Gilman, *ibid.* **264**, 409 (1989).
30. D. Benjamin, D. W. Markby, H. R. Bourne, I. D. Kuntz, unpublished data.
31. W. Gilbert, *Nature* **271**, 501 (1978).
32. T. Kozasa, H. Itoh, T. Tsukamoto, Y. Kaziro, *Proc. Natl. Acad. Sci. U.S.A.* **85**, 2081 (1988); H. Itoh *et al.*, *J. Biol. Chem.* **263**, 6656 (1988).
33. T. E. Creighton, in *Proteins: Structures and Molecular Properties* (Freeman, New York, 1993), p. 307.
34. M. V. Milburn *et al.*, *Science* **247**, 939 (1990).
35. E. F. Pai *et al.*, *EMBO J.* **9**, 2351 (1990).
36. F. Jurnak, *Science* **230**, 32 (1985); M. Kjeldgaard and J. Nyborg, *J. Mol. Biol.* **223**, 721 (1992); H. Berchtold *et al.*, *Nature* **365**, 126 (1993).
37. Intrinsic GTP hydrolysis by Ras proceeds by direct nucleophilic attack of water on the γ -phosphate of GTP [J. Feuerstein, R. S. Goody, M. R. Webb, *J. Biol. Chem.* **264**, 6188 (1989)]. Proposed mechanisms include activation of water by glutamine 61 (35) and transition state stabilization by several residues [G. G. Privé *et al.*, *Proc. Natl. Acad. Sci. U.S.A.* **89**, 3649 (1992)]. Possible

- mechanisms of GAP action include stabilizing the pentavalent phosphorus transition state, protonating the leaving group GDP, increasing the nucleophilicity of attacking water, bypassing a proposed rate-limiting conformational change [S. E. Neal, J. F. Eccleston, M. R. Webb, *Proc. Natl. Acad. Sci. U.S.A.* **87**, 3562 (1990)], or changing the chemical mechanism to include a phosphorylated enzyme intermediate.
38. G. G. Brownbridge, P. N. Lowe, K. J. M. Moore, R. H. Skinner, M. R. Webb, *J. Biol. Chem.* **268**, 10914 (1993); R. H. Skinner *et al.*, *ibid.* **266**, 14163 (1991).
39. D. Diekmann *et al.*, *Nature* **351**, 400 (1991); B. Rubinfeld *et al.*, *Cell* **65**, 1033 (1991); M. Strom, P. Vollmer, T. J. Tan, D. Gallwitz, *Nature* **361**, 736 (1993); T. Yoshihisa, C. Barlowe, R. Schekman, *Science* **259**, 1466 (1993).
40. N. Green *et al.*, *Cell* **23**, 477 (1982).
41. J. D. Robishaw, M. D. Smigel, A. G. Gilman, *J. Biol. Chem.* **261**, 9587 (1986).
42. D. T. Jones and R. R. Reed, *ibid.* **262**, 14241 (1987).
43. All Ralph and Gail derivatives were constructed by PCR from rat α_s cDNA (42) and confirmed by DNA sequencing. For Gail constructs, the sequence, MGADVPDYASN-, was introduced as an NH₂-terminal extension and a stop codon was created at the desired position; a restriction site for Nco I was created at the initiating methionine and sites for Bam HI and Sma I were created after the stop codon. The plasmids pBN-107 and pBN-184 encoded G-2 and G-2-R201C, respectively, as Nco I-Bam HI inserts in pET3d [F. W. Studier, A. H. Rosenberg, J. J. Dunn, J. W. Dubendorff, *Methods Enzymol.* **185**, 60 (1990)]; pBN-180 encoded G-2 as an Xba I-Sma I insert in pCMV4 [S. Andersson, D. L. Davis, H. Dahlback, H. Jornvall, D. W. Russell, *J. Biol. Chem.* **264**, 8222 (1989)]; the insert also included the ~45-bp Xba I-Nco I fragment of pET3d as 5' untranslated sequence. pCMV4 derivatives encoding other Gail proteins were constructed similarly. For Ralph derivatives, internal deletions in α_s cDNA were created by PCR and cloned into pGRS (18). The plasmid pBN-179 encoded R-1-Q227L as an Xba I-Hin dIII insert from pGRS cloned into the polylinker of a derivative of pSM [M. H. Brodsky, M. Warton, R. M. Myers, D. R. Littman, *J. Immunol.* **144**, 3078 (1990)]. Hexahistidine-tagged R-2 and α_s included the NH₂-terminal extension MGAHHHHHH, followed by the coding sequence of α_s (MGCL...), with a restriction site for Nco I at the initiating methionine of the fusion protein. The plasmids pBN-181, pBN-182, and pBN-183 were constructed by cloning the coding sequences for H₆-R-2, H₆- α_s , and G-2, respectively, into the Nco I and Sma I sites of pAcC13- α_2 [S. Munemitsu *et al.*, *Mol. Cell. Biol.* **10**, 5977 (1990); P. T. Wilson and H. R. Bourne, unpublished data]. The plasmids pBN-179, pBN-181, and pBN-182 all included ~180 bp of 3' untranslated sequence up to the 3' Hin dIII site in rat α_s cDNA (18, 42).
44. G-2 was expressed in *E. coli* BL21(DE3)pLysS with vectors pBN-107 or pBN-184 (43). Cells were grown at 37°C in M9 medium supplemented with chloramphenicol (30 μ g/ml) and carbenicillin (50 μ g/ml) and induced with isopropyl-thiogalactoside for 3 to 4 hours (43). The cells were collected by centrifugation and stored at -70°C. The following procedures were done at 4°C or on ice: Cells (~1 g per 4 ml buffer) were thawed and lysed by resuspension in Q buffer [50 mM bis-tris (bis[2-hydroxyethyl]imino-tris[hydroxymethyl]-methane) (pH 6.0), 1 mM EDTA, 2 mM 2-mercaptoethanol, 0.1 mM phenylmethylsulfonyl fluoride, and 1 μ g/ml pepstatin A]. The extract was clarified by addition of 5 mM MgCl₂ and deoxyribonuclease I followed by centrifugation. The freeze-thaw lysis was repeated and the lysates were pooled. G-2 was monitored during purification as an abundant 16-kD protein on SDS-polyacrylamide gels (15% stained with Coomassie blue. G-2 was purified on a Q Sepharose Fast Flow (Pharmacia) column eluted with a linear gradient of 0 to 0.5 M NaCl in Q buffer, a Sephacryl S200 High Resolution (Pharmacia) column equilibrated in S buffer [50 mM tris-Cl (pH 7.2), containing 1 mM EDTA and 2 mM 2-mercaptoethanol], and a Biogel HTP hydroxylapatite (Bio-Rad) column eluted with a linear gradient of 0 to 25 mM potassium phosphate (pH 7.2) in S buffer. Purified G-2 was concentrated in a Centrprep-10 (Amicon) to ≥ 2 mg/ml and stored at -70°C in S buffer or HEB [50 mM Na-Hepes (pH 8.0) 0.1 mM EDTA, and 2 mM 2-mercaptoethanol]. The concentration of G-2 was determined from the extinction coefficient at 280 nm (1.0 cm² mg⁻¹) (46). Final yields ranged from 3 mg to 15 mg per liter of culture with greater than 98% purity as judged by SDS-PAGE (Fig. 2B).
- Purification of H₆-R-2. Sf9 cells were maintained in shaker cultures at 28°C in Sf-900II serum-free media (Gibco-BRL) with fungizone, according to the manufacturer's instructions. Recombinant viruses were generated by co-transfection of the transfer vectors and linearized AcNPV baculovirus into Sf9 cells by lipofection (Invitrogen). Viruses were amplified and plaque-purified as described (47). Protein immunoblotting was used to detect recombinant protein (Fig. 2B). Sf9 cells were co-infected with viruses expressing H₆-R-2 and G-2 (multiplicity of infection ≈ 5) and grown for 30 to 36 hours in 150-ml shaker cultures or 500-ml spinner cultures. The cells were collected by centrifugation and frozen at -70°C. Cells (~2.5 $\times 10^7$ cells/ml buffer) were lysed by thawing in N buffer [20 mM tris-Cl (pH 8.0), 2 mM 2-mercaptoethanol, 1 mM MgCl₂, 10 μ M GDP, 0.1 mM phenylmethylsulfonyl fluoride, and 1 μ g/ml pepstatin A, 4 μ g/ml leupeptin, and 8 μ g/ml aprotinin], and cell debris was removed by centrifugation. The extract was adjusted to 50 mM tris-Cl (pH 8.0), 200 mM NaCl, and 10 mM imidazole-Cl (pH 7.4) and then mixed (1 ml resin/15 ml extract) as a slurry for 1 hour with Ni-NTA resin (Qiagen) equilibrated in N buffer containing 50 mM tris-Cl (pH 8.0), 10 mM imidazole-Cl (pH 7.4), and 200 mM NaCl. The resin was then transferred to a column and washed with 10 bed volumes of equilibration buffer. R-2 was eluted with I buffer [150 mM imidazole-Cl (pH 7.4), 200 mM NaCl, 2 mM 2-mercaptoethanol, 1 mM MgCl₂, 10 μ M GDP, 0.1 mM phenylmethylsulfonyl fluoride, and 0.1 μ g pepstatin A]. In some cases, the eluate from the Ni-NTA column was concentrated using a Centrprep-10. The sample was desalted into HEB with a PD-10 column (Pharmacia) and stored at -70°C in HEB with bovine serum albumin (4 mg/ml). For some experiments, H₆-R-2 was further purified on a second Ni-NTA column. The concentration of active H₆-R-2 was determined by GTP- γ -S binding at 400 nM GTP- γ -S and 2.5 μ M G-2 in G buffer. This assay is specific and quantitative because: (i) GTP- γ -S binding was largely dependent on added G-2 (Fig. 4A) and was saturable with respect to both G-2 and GTP- γ -S (Fig. 4, A and B); and (ii) GTP- γ -S dissociation was slow under the filtration conditions used. From Coomassie-stained polyacrylamide gels with α_s as a standard, we estimate that the R-2 preparation was $\geq 10\%$ pure and that $\geq 20\%$ of the total R-2 bound GTP- γ -S. Samples of H₆-R-2 were thawed just before use and held on ice with stabilizing agents (glycerol, GTP- γ -S, or G-2) added as appropriate for each assay.
- H₆- α_s was purified from Sf9 cells infected with recombinant virus with Ni-NTA resin as described for H₆-R-2. The sample was desalted into buffer containing 50 mM tris-Cl (pH 8.0), 1 mM EDTA, and 2 mM 2-mercaptoethanol, and further purified on a Q Sepharose Fast Flow column eluted with a linear gradient of 0 to 350 mM NaCl in the same buffer. Fractions containing H₆- α_s were located by GTP- γ -S binding, pooled, and frozen as described for H₆-R-2. This preparation was $>90\%$ pure as judged by SDS-polyacrylamide gels stained for total protein (Fig. 2B). H₆- α_s concentration was determined by GTP- γ -S binding activity at 1 μ M GTP- γ -S in G buffer without glycerol (Fig. 4).
45. M. J. Levis and H. R. Bourne, *J. Cell Biol.* **119**, 1297 (1992).
46. M. L. Elwell and J. A. Schellman, *Biochim. Biophys. Acta.* **494**, 367 (1977).
47. M. D. Summers and G. E. Smith, *A Manual of Methods for Baculovirus Vectors and Insect Cell Culture Methods* (Texas Agricultural Experiment Station Bulletin 1555, College Station, TX, 1987).
48. J. K. Northup, M. D. Smigel, A. G. Gilman, *J. Biol. Chem.* **257**, 11416 (1982).
49. We thank D. Eggers and B. Kharrazi for assistance with some experiments; T. Mitchison, F. Cohen, and I. D. Kuntz for reading the manuscript; and P. Wilson, T. Iiri, M. Levis, C. Berlot, and D. Benjamin for advice and encouragement. Supported by a grant from the March of Dimes and NIH grants GM27800 and CA54427 (H.R.B.) and 5F32-GM13918 (D.W.M.). R.O. is a fellow of the Helen Hay Whitney Foundation.

18 October 1993; accepted 22 November 1993

Linearity of Summation of Synaptic Potentials Underlying Direction Selectivity in Simple Cells of the Cat Visual Cortex

Bharathi Jagadeesh,* Heidi S. Wheat, David Ferster†

Intracellular recordings from simple cells of the cat visual cortex were used to test linear models for the generation of selectivity for the direction of visual motion. Direction selectivity has been thought to arise in part from nonlinear processes, as suggested by previous experiments that were based on extracellular recordings of action potentials. In intracellular recordings, however, the fluctuations in membrane potential evoked by moving stimuli were accurately predicted by the linear summation of responses to stationary stimuli. Nonlinear mechanisms were not required.

Computational processes in the brain depend critically on the mechanisms by which single neurons integrate their synaptic inputs. Cells that use nonlinear synaptic mechanisms, such as shunting inhibition or synaptic facilitation, are capable of far more complex computations than cells that are limited to linear mechanisms. In the primary

visual cortex, it is an important goal to delineate those computational mechanisms that make neurons selective to visual features such as orientation and direction of motion (1-4).

Direction selectivity is a receptive field property for which models of linear summation of synaptic potentials have been rigor-